DOI: 10.13009/EUCASS2019-482

Tunable Diode Laser Absorption Tomography for characterization of chemical species in aeronautical flames

Vincent Corbas, Frédéric Champagnat, Guy Le Besnerais, Ajmal Mohamed
ONERA 6 Chemin de la Vauve aux Granges 91120 Palaiseau
vincent.corbas@live.fr, Frederic.champagnat@onera.fr, guy.le_besnerais@onera.fr, ajmal_khan.mohamed@onera.fr

Abstract

Chemical species densities like H_2O and CO_2 and thermodynamic data like pressure and temperature are key parameters characteristic of a combustion reaction. Measurements of these parameters can be used in numerical simulations in order to improve engine design and efficiency. This article present an extension of the Tunable Diode laser Absorption Spectroscopy (TDLAS) by adding of a tomography technique in order to obtain two dimensional mapping of chemical densities, pressure and temperature in aeronautical flames. This article presents the principle of the reconstruction method and several tests of the method through simulations and experiments.

Introduction

The absorption spectroscopy is a well-known and efficient method used to characterize chemical species density and thermodynamic parameters in gas and more particularly in combustion flames. In a homogenous medium, this technique provides high precision measurements. However, in an inhomogeneous medium like a flame this precision is deteriorated. Indeed, the measurements are integrated on the beam path and the spatial resolution within this path is lost. On the other hand, spatial resolution can be recovered by using several lasers beams acquired at different positions and angles around the flame and a tomographic reconstruction on the TDLAS spectral data. The combination of the spectral measurement from the TDLAS method with a tomographic algorithm is called Tunable Diode laser Absorption Tomography (TDLAT). TDLAT provides two dimensional maps of chemical density, pressure and temperature. However, in order to work properly a tomographic algorithm needs several measurement beams at many different positions and angles. This is an issue since combustion benches usually lack of optical access. These limited accesses have to be accounted for in the tomographic algorithm to obtain correct reconstructions.

First, this paper presents the theoretical principles of the TDLAT method. Second, the experimental device is described along with its associated constraints, and their impact on tomographic reconstruction results is discussed. Then, numerical simulations results and experimental reconstructions made on a McKenna Burner are presented. Finally, conclusions about the efficiency of the developed are drawn and improvements on the reconstruction method code and experimental device are proposed.

1. Tunable Diode Laser Absorption Tomography principle

The principle of the TDLAS method is based on the Beer-Lambert law that describes, for a particular wave-number range, the attenuation of a laser beam intensity when it goes through a gaseous medium as a function of the chemical density species, pressure and temperature [1]. When considered as a function of the wave-number, this attenuation curve is called an absorption spectrum. Tomography uses a large number of these curves, referred to as projection or projection spectra, to reconstruct a two dimensional mapping of the involved physical parameters. Each of these parameters (pressure, temperature and species concentration) are modelled as piecewise constant functions defined over a grid of pixels recovering the whole flame section, see Figure 1.

DOI: 10.13009/EUCASS2019-482

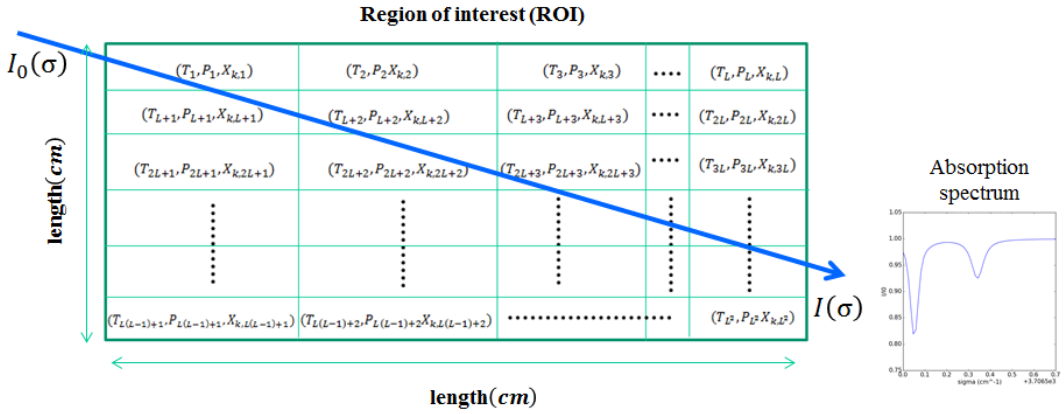

Figure 1: Modelling a flame section as a pixel grid. In each pixel, the density of chemical species, the pressure and the temperature are assumed constant

According to the Beer-Lambert law, the attenuation of the laser beam intensity indexed j is described by equation (1):

$$\frac{I_j(\sigma)}{I_0(\sigma)} = \exp\left(-\sum_l \sum_{kr} S(\sigma_{krl}, T_l).X_{kl}.f(\sigma-\sigma_{krl}, P_l, T_l)w_{jl}\right) \tag{1}$$

With σ the wave-number (cm^{-1}), l the pixel index, L^2 the total number of pixels in the region of interest, k the chemical species isotope, r the absorption line of this isotope, X_{kl} the density of the isotope k in the pixel l (molecule.cm^{-3}), P_l the pressure inside the pixel l (bar), T_l the temperature in the pixel l (K), w_{jl} the intersection length between the beam j and the pixel l (cm), $f(\sigma-\sigma_{krl}, P_l, T_l)$ the Voigt profile (cm) which describe the line shape as a function of the pressure and temperature and $S(\sigma_{krl}, T_l)$ the line strength (cm^{-1}.molecule^{-1}.cm^2) proportional to the temperature. The evolution of the line strength according to temperature is given by equation (2):

$$S(\sigma_{krl}, T_l) = S(\sigma_{krl}, T_0).\frac{Q_k(T_0)}{Q_k(T_l)}.\frac{1-\exp\left(-\frac{hc}{k_B}.\frac{\sigma_{krl}}{T_l}\right)}{1-\exp\left(-\frac{hc}{k_B}.\frac{\sigma_{krl}}{T_0}\right)}.\exp\left(-\frac{hc}{k_B}E_{kr}\left(\frac{1}{T_l}-\frac{1}{T_0}\right)\right) \tag{2}$$

With Q_k the partition function of the isotope k, $T_0 = 296\ K$ the atmospheric temperature, h the Planck constant (J.s), c the speed of light (cm.s^{-1}), k_B the Boltzmann constant (J.K^{-1}), E_{kr} the internal energy (cm^{-1}) of the line r of the isotope k. Values of $S(\sigma_{krl}, T_0)$ and of Q_k are given for each molecules in the database HITRAN [2]. The Voigt profile is the convolution of a Lorentzian profile with a Doppler profile which is calculated by the numerical approximation of Hui et al. [3].

For a tomography calculation, we define the local absorption of a pixel indexed l noted $\alpha_l(\sigma)$ expressed in cm^{-1}. This value is the contribution of pixel l to the absorption of the beam intensity. It is given by equation (3):

$$\alpha_l(\sigma) = \sum_{kr} S(\sigma_{krl}, T_l).X_{kl}.f(\sigma-\sigma_{krl}, P_l, T_l) \tag{3}$$

The calculation of a projected spectrum for a particular beam by taking account of all the pixels crossed by the beam path is done by a matrix product given by equation (4):

$$\boldsymbol{p_j(\sigma)} = ln\left(\frac{I_j(\sigma)}{I_0(\sigma)}\right) = w_{jl}.\boldsymbol{\alpha_l(\sigma)} \tag{4}$$

With $\boldsymbol{p_j(\sigma)}$ the projected spectrum of the beam j as a function of the wave-number σ, $\boldsymbol{\alpha_l(\sigma)}$ the local absorption in the pixel l as a function of the wave-number and $\boldsymbol{w_{jl}}$ a matrix that contain intersections lengths between each beam j and each pixel l. Such matrix $\boldsymbol{W}$ is used currently in computed tomography methods like Algebraic Reconstruction Technique (ART) and it is called the system matrix [4]. Then, by knowing the trajectory of each beam, it is possible

DOI: 10.13009/EUCASS2019-482

to know each coefficient of the system matrix $\boldsymbol{W}$and so to compute every spectrum $\boldsymbol{p_j(\sigma)}$ that it is likely to be measured in the region of interest.

The objective of the tomographic method is to retrieve the contributions $\boldsymbol{\alpha_l(\sigma)}$ and to deduce values of $\boldsymbol{P_l, T_l}$ and $\boldsymbol{X_{kl}}$. The TDLAT method first measures several absorption projected spectra around the flame with a known beam arrangement. These spectra are gathered in a vector $\boldsymbol{p_{mes}}$. sApplying the system matrix on initial $\boldsymbol{(T_l, P_l, X_{kl})}$ profiles provides predicted projections gathered in a vector called $\boldsymbol{p_{calc}(T_l, P_l, X_{kl})}$. Then, adopting an iterative least-squares minimization algorithm, the initial profiles of pressure, temperature and densities are corrected iteratively until minimization of the mean squared error between the computed and measured spectra. The iterative approach is illustrated on Figure 2. One iteration of this non linear tomographic reconstruction [5] is given by the equation (5):

$$C = \left\| \boldsymbol{p_{mes}} - \boldsymbol{p_{calc}(T_l, P_l, X_{kl})} - \frac{\boldsymbol{\delta p_{calc}(T_l, P_l, X_{kl})}}{\boldsymbol{\delta(T_l, P_l, X_{kl})}} \boldsymbol{(\delta T_l, \delta P_l, \delta X_{kl})} \right\|^2 \tag{5}$$

With C the first-order expanded linear criterion which is to be minimized at the current iteration, $\boldsymbol{p_{mes}}$ the measured projected spectra, $\boldsymbol{p_{calc}(T_l, P_l, X_{kl})}$ the projected spectra calculated numerically with initialized profiles of pressure $\boldsymbol{P_l}$, temperature $\boldsymbol{T_l}$ and densities $\boldsymbol{X_{kl}}$, $\frac{\boldsymbol{\delta p_{calc}(T_l, P_l, X_{kl})}}{\boldsymbol{\delta(T_l, P_l, X_{kl})}}$ the partial derivatives of calculated spectra as a function of $\boldsymbol{(T_l, P_l, X_{kl})}$ in each pixel gathered in a Jacobian matrix, $\boldsymbol{(\delta T_l, \delta P_l, \delta X_{kl})}$ incremental variations of pressure, temperature and densities to add to the initials in order to fit calculated spectra with measured spectra.

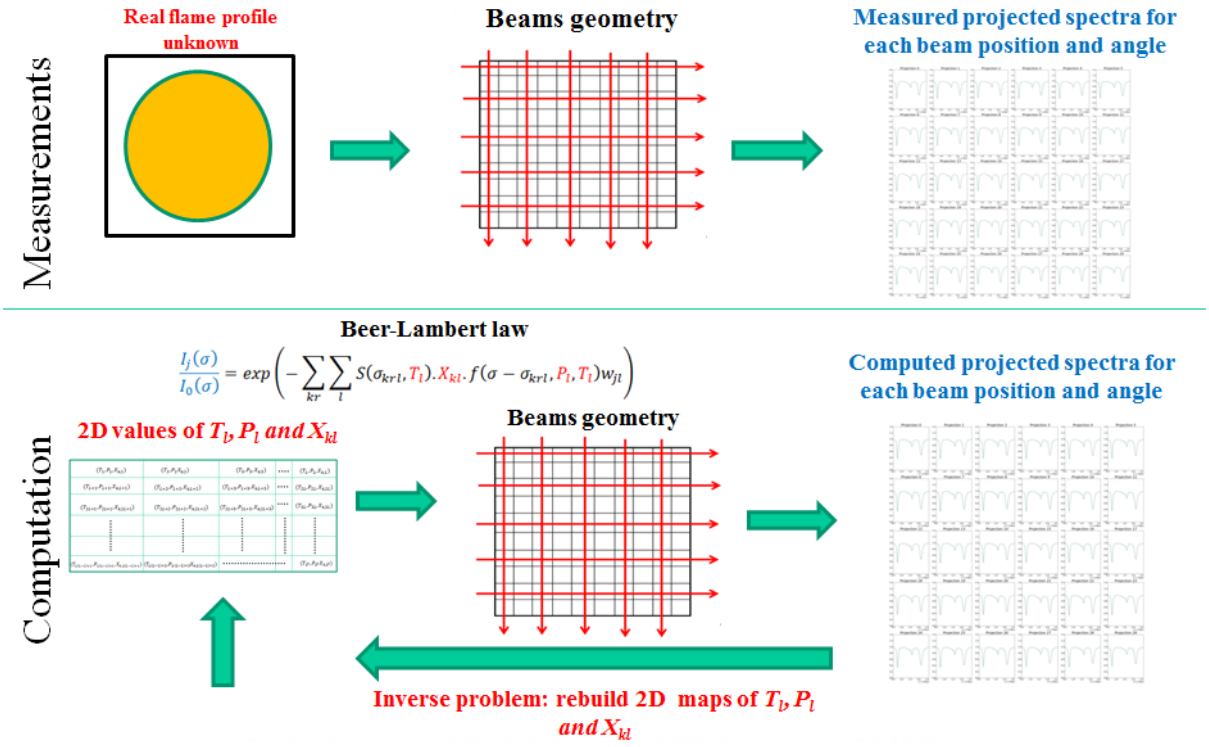

Figure 2: TDLAT algorithm principle

2. Regularisation of the TDLAT algorithm

The least-squares algorithm presented in the previous section needs enhancements in order to work properly on real data. First, because of the limited number of measured beams. Indeed, this method has to be used on combustion benches which allow only very few optical access. Moreover, the TDLAS spectrometers are mostly constituted of fibered lasers which imply fiber focalization and difficulty to maintain the required power level from the source to the detectors. This let only few possibilities to divide the optical power into different beams. A second major issue is that experimental spectra are always contaminated by noise. These limitations on the data lead to unexploitable

DOI: 10.13009/EUCASS2019-482

results if one relies on the previously describe iterative least-squares method. The fundamental reason is that tomography is a ill-posed problem, or, in other terms, that the system matrix is ill-conditioned : lack of data and measurement noise then translate into large perturbations on the reconstructed profiles. To solve these problems, a solution currently used in linear tomography is Tikhonov regularization [6]. The basic idea of Tikhonov regularization is to add a smoothness penalty to the least-squares data term. It means a prior information on the continuity of pressure, temperature and species density in the flame which is justified physically by the thermal and mass diffusion. As a consequence, values of pressure, temperature and density are not truly different between two neighbor's pixels. It is implemented in the equation (5), by addition of regularization penalty terms $\left(\boldsymbol{R_P}, \boldsymbol{R_T}, \boldsymbol{R_{X_k}}\right)$ which are proportional to the sum of squared horizontal and vertical gradients on the pixel grid applied on pressure, temperature and chemicals densities:

$$C = \left\| \boldsymbol{p_{mes}} - \boldsymbol{p_{calc}}(\boldsymbol{T_l}, \boldsymbol{P_l}, \boldsymbol{X_{kl}}) - \frac{\boldsymbol{\delta p_{calc}}(\boldsymbol{T_l}, \boldsymbol{P_l}, \boldsymbol{X_{kl}})}{\boldsymbol{\delta}(\boldsymbol{T_l}, \boldsymbol{P_l}, \boldsymbol{X_{kl}})} (\boldsymbol{\delta T_l}, \boldsymbol{\delta P_l}, \boldsymbol{\delta X_{kl}}) \right\|^2 + \lambda_P \boldsymbol{R_P} + \lambda_T \boldsymbol{R_T} + \lambda_{X_k} \boldsymbol{R_{X_k}} \quad (6)$$

With:

$$\begin{cases} R_P = \|D_x.P\|^2 + \|D_y.P\|^2 \\ R_T = \|D_x.T\|^2 + \|D_y.T\|^2 \\ R_{X_k} = \|D_x.X_k\|^2 + \|D_y.X_k\|^2 \end{cases} \quad (7)$$

With $\boldsymbol{D_x}$ the horizontal derivative matrix, $\boldsymbol{D_y}$ the vertical derivative matrix and $\left(\boldsymbol{\lambda_P}, \boldsymbol{\lambda_T}, \boldsymbol{\lambda_{X_k}}\right)$ weighting coefficients that tune the regularization impact on the tomographic algorithm. Indeed, the regularization need to be strong enough to control the effect of noise on the measurement but not too much strong to keep the measurements information important in the reconstruction algorithm. It is then necessary to optimize the regularization parameters which is a difficult and still open issue when dealing with nonlinear inversion problems such as TDLAT. But first, we have to define first the conditions of the tomographic reconstructions which are the beam arrangement, the nature of flame environment and the experimental constraints of the TDLAS measurements.

3. Experimental device and constraints on spectral inversion

We will explain in this part the functioning of the TDLAS spectrometer used in our experiments, the calibration techniques and the environment of the measurement on an experimental MacKenna burner. A TDLAS measurement is done with an absorption spectrometer. Its principle is illustrated on Figure 3.

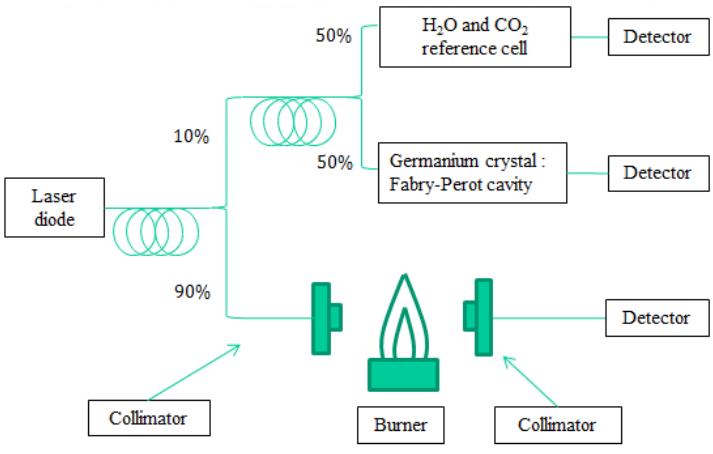

Figure 3: Principle of a TDLAS spectrometer.

Such spectrometer is generally composed of a laser diode tunable in wavelength. In the current case, the diode is tunable between 3706,3 cm^{-1} and 3707,0 cm^{-1} in order to acquire absorption line of H_2O and CO_2 detectable enough in the thermochemical conditions of the study. Laser instability and measurement uncertainty necessitate a precise spectral calibration for each spectrum acquired. Around 10% of the laser power is taken for this purpose. These 10% are divided in two parts that provide two calibration spectra used to calibrate the spectral resolution, see

DOI: 10.13009/EUCASS2019-482

Figure 4. The first part passes through a reference cell which contains H_2O and CO_2 vapor at $10\ kPa$ and at a temperature of $300\ K$, providing an absorption spectrum with identified absorption lines used as a reference. Low pressure leads to very thin absorption lines, which spectral position can be very precisely estimated. The second part of the light passes through a germanium crystal with polished faces at λ/10 used as Fabry-Pérot cavity to produce an interference figure (Figure 4). Interference lines separations in wave-number are known and dependent of physical properties of the cavity. The combination of these two spectral markers allows the absolute spectral calibration of measured spectra.

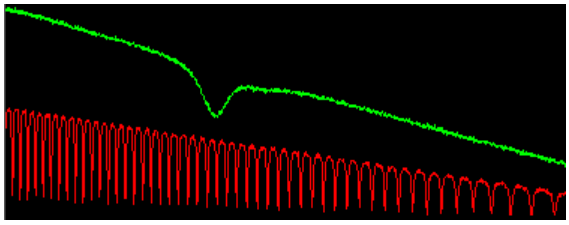

Figure 4: Calibration spectra: reference line in low pressure cell in green and interference figure from the Fabry-Pérot cavity in red

The third part of the signal representing 90% of the total power is sent into the flame with optical fibbers connected to off-axis collimators. In the case of present study, the considered flame is a methane/air McKenna burner which produces a flat flame stable in time and with a circular symmetry. These conditions are obtained for particular conditions of flows parameters (Figure 5).

(a) (b)

Figure 5: Image of (a) burner McKenna and (b) of a configuration of stable flat flame for flows of 20mL/s of air and 2mL/s of methane

Moreover, before going into the flame, the beam is passing through atmosphere that is containing H_2O and CO_2 vapor visible on the acquired spectra. So, in order to measure the effect of vapors inside the flame, it is essential to suppress the atmosphere contributions on absorptions lines first, an operation called “suppression of the spectral envelop”. It is based on the acquisition of a reference spectrum without the flame at the same position and angle so as to keep the same beam path (Figure 6).

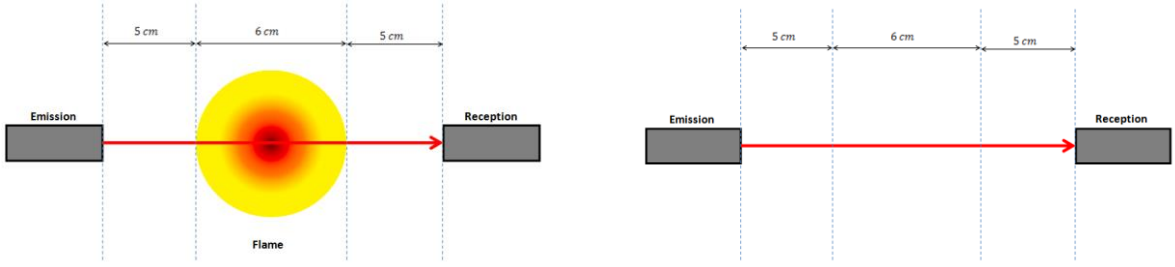

(a) (b)

Figure 6: Measurement of the atmospheric contribution on absorption spectra, (a) measurement of the contributions of the flame and of the atmosphere and (b) quantification of the atmosphere contribution to suppress it on the acquired spectrum

As a result, the contribution of the ambient air is quantified and it is possible to suppress this contribution on the spectrum acquired in the flame (Figure 7).

DOI: 10.13009/EUCASS2019-482

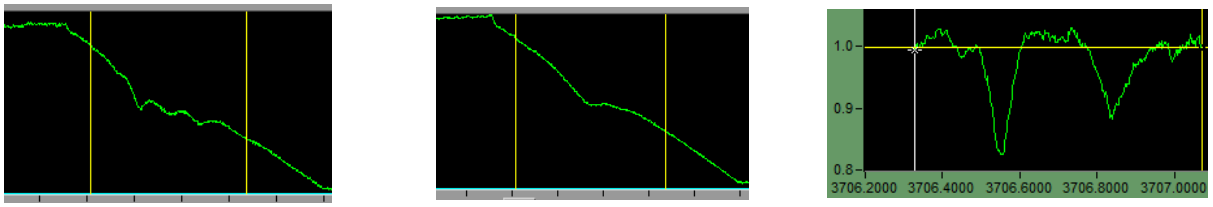

(a) (b) (c)

Figure 7: Suppression of the spectrum envelop, (a) spectrum acquired with the flame and the atmosphere slice, (b) spectrum acquired without which quantify the atmospheric contribution and (c) the final spectrum without atmospheric contributions

Suppression of the spectral envelop modifies the final spectrum used to the spectral inversion. Indeed, on the spectrum shown in Figure 7, it is possible to see three main absorptions lines: two H_2O lines and one CO_2 line between the two H_2O lines. Another consequence is the suppression of the CO_2 line. So it means that the spectrometers sees the CO_2 specie only on in the atmosphere around the flame but not inside. As a result, in the others parts of the study, we will consider on numerical simulations and experimentations that there no CO_2 visible in the flame. The reconstruction will only concern the H_2O density. Moreover, the MacKenna burner makes a flame in the atmospheric pressure conditions. The pressure in the flame fluctuate around the atmosphere pressure but because of the noise and line deformations, the spectra are not very sensitive to the pressure and so we assume pressure constant and equal to atmospheric pressure in the entire the region of interest. As a result, the model of tomography reconstruction will be done only on H_2O density and temperature profiles. The equations (6) and (7) then reduce to:

$$C = \left\| \boldsymbol{p_{mes}} - \boldsymbol{p_{calc}}(\boldsymbol{T_l}, \boldsymbol{X_{kl}}) - \frac{\boldsymbol{\delta p_{calc}}(\boldsymbol{T_l}, \boldsymbol{X_{H_2O,l}})}{\boldsymbol{\delta}(\boldsymbol{T_{l,}}, \boldsymbol{X_{H_2O,l}})} (\boldsymbol{\delta T_l}, \boldsymbol{\delta X_{H_2O,l}}) \right\|^2 + \lambda_T \boldsymbol{R_T} + \lambda_{X_{H_2O}} \boldsymbol{R_{X_{H_2O}}} \tag{8}$$

With:

$$\begin{cases} R_T = \|D_x.T\|^2 + \|D_y.T\|^2 \\ R_{X_{H_2O}} = \left\|D_x.X_{X_{H_2O}}\right\|^2 + \left\|D_y.X_{X_{H_2O}}\right\|^2 \end{cases} \tag{9}$$

4. Tomography scanning device

The quality of a tomographic reconstruction is depending not on only on the number of beams available but also on their positions and their angles around the region of interest. First of all, because of the difficulties to keep enough light power in fibered path, only a few beams can be used to do correct measurements in the flame. So it is necessary to find a way to multiply the number of beams while keeping enough optical power. As a result, the tomographic device was oriented to choose measurement with scanning. Different possibilities have been studied but the better and chosen one is a configuration with five beams and with a rotational scanning. This configuration uses the rotation of a metallic crown whose centre is shifted from the flame centre. The scanning is done on amplitude of 90° around the flame. The amplitude of the rotation cannot be larger because of the tension that could be created on optical fibres. Then by choosing optimal positions of sources and detectors, it is possible to obtain the reproduction of five fan-beams around the flame (Figure 8). This beam arrangement allows the possibilities to see the flame in a lot of angles and positions. This beam arrangement is first considered within a numerical study to optimize the regularisation parameters on the model of equations (8) and (9) . Then, the same configuration will be tested experimentally on the MacKenna burner.

DOI: 10.13009/EUCASS2019-482

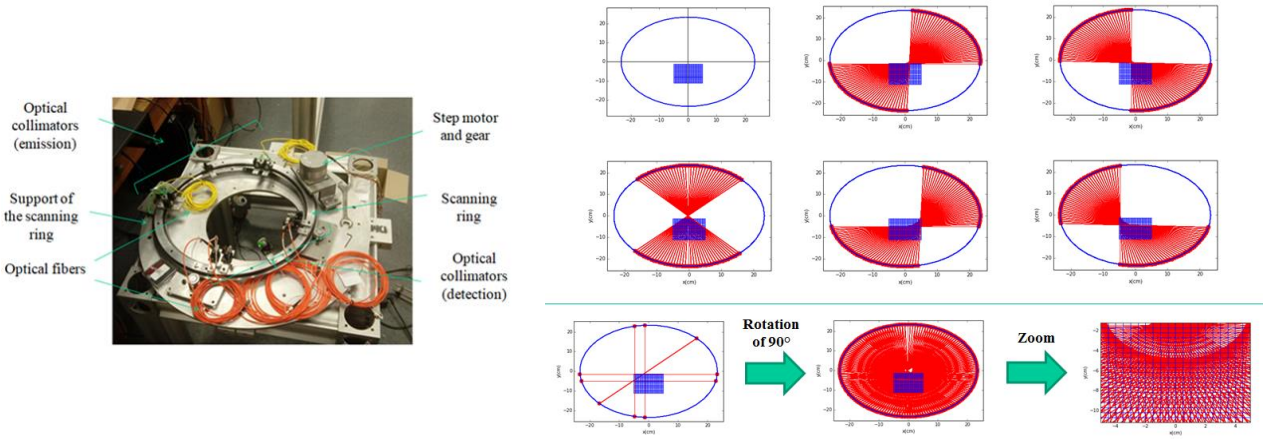

(a) (b)

Figure 8: (a) Image of the rotation scanning device and (b) reproduction of a fan-beam measurement configuration around the region of interest

5. Optimisation of regularisation parameters on the studied model

In this part we will study in simulation the impact of the regularization parameters on the reconstruction quality. The objective is to study the impact of the regularization parameters on the tomographic reconstruction when two parameters are reconstructed and when one of them has a non-linear effect on the measured data. To do that, we will first define two profiles X_{H_2O} and T to study. These profiles are two images of 20x20 pixels representing a two dimensional Gaussian profiles which is considered as a rough approximation of the MacKenna burner shape (Figure 9).

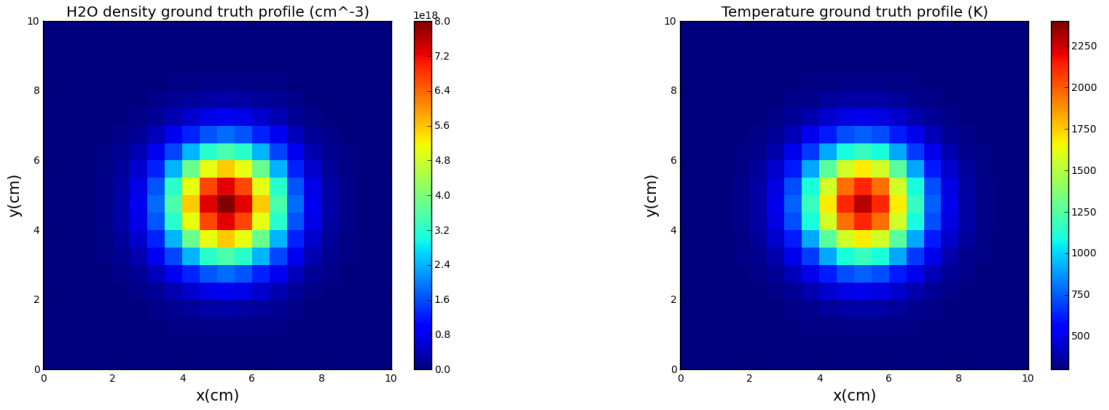

(a) (b)

Figure 9: Simulated two-dimensional phantoms reproducing the shape of (a) a H_2O density profile and (b) a temperature profile of a MacKenna burner

The quality of the tomographic reconstruction is dependent of the regularization parameters. The two main problems in the case of the TDLAT are the non-linearity of the problem and the multi-parameter optimization. Commonly, in a linear tomographic problem, the method used is the L-curve representation [7]. It consists to draw the regularization terms (9) as a function of the data match score for several λ values. The data match score M is quantified by the residuals between measured spectra and reconstructed spectra:

$$M = \left\| \boldsymbol{p}_{mes} - \boldsymbol{p}_{calc}(\boldsymbol{T}_l, \boldsymbol{X}_{kl}) \right\|^2 \tag{10}$$

The regularization term is quantified on the H_2O density and the temperature by the terms defined in equation (9).

DOI: 10.13009/EUCASS2019-482

The L-curve representation consists to draw a regularization term $R_{X_{H_2O}}$ or R_T for several values of $\lambda_{X_{H_2O}}$ or λ_T as a function of the data match M.In practice, this technique did not proved to work well here, in particular due to the high non linearity of $\boldsymbol{p}_{\text{calc}}$ with respect to temperature.. As a result, we choose another approach to optimize the regularization. We choose to study a normalized error between the phantoms (called the ground truth profiles) and the rebuilt ones as a function of the regularization parameter. These errors are expressed as follows:

$$\begin{cases} e_{X_{H_2O}} = \dfrac{\left\| X_{H_2O_{gt}} - T_{rec} \right\|^2}{\left\| X_{H_2O_{gt}} \right\|^2} \\ e_T = \dfrac{\left\| T_{gt} - T_{rec} \right\|^2}{\left\| T_{gt} \right\|^2} \end{cases} \tag{11}$$

If we draw the difference between $e_{X_{H_2O}}$ as a function of $\lambda_{X_{H_2O}}$ (Figure 10 (a)), it is possible to see that the $\lambda_{X_{H_2O}} = 1{,}0.10^{-7}$ coefficient gives the best reconstruction with the least difference between phantom and rebuilt profile. The minimum of $e_{X_{H_2O}}$ is given the best $\lambda_{X_{H_2O}}$ to choose in order to do an experimental reconstruction in the same conditions of beam arrangement and noise. The same operation can be done by representing e_T as a function of λ_T. This curve represented on Figure 10 (b) show that the value of $\lambda_T = 3{,}0.10^{-8}$ give the best error value.

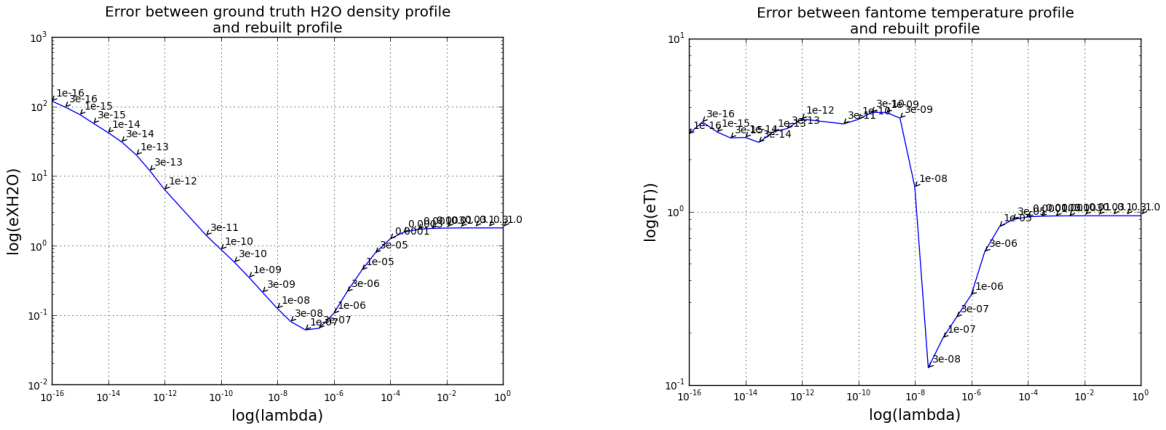

(a) (b)

Figure 10: Reconstructions errors as a function of the λ coefficient on H_2O density and temperature reconstruction

As a result, this optimisation gives separately a couple of optimal regularisation coefficient $\left(\lambda_{X_{H_2O}}, \lambda_T\right)$. With Figure 11 and Figure 12, it is possible to illustrate that these coefficients give the best reconstruction results when they are optimal. If they are too low the reconstructions are too noisy diverging and when it is too large , reconstructions are too smooth.

DOI: 10.13009/EUCASS2019-482

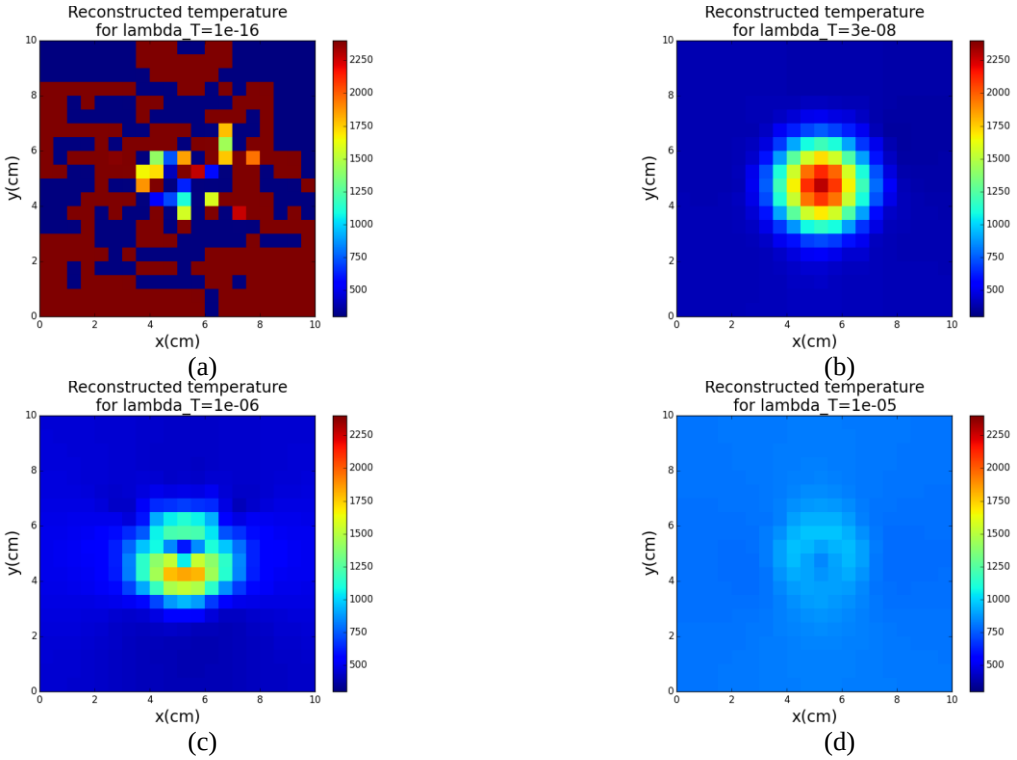

(a) (b) (c) (d)

Figure 11: Different results of tomographic reconstructions of the temperature with fixed density for different values of regularisation coefficient: (a) with $\lambda_T = 1{,}0.10^{-16}$ a too low, (b) $\lambda_T = 3{,}0.10^{-8}$ the optimal value, (c) $\lambda_T = 1{,}0.10^{-6}$ and (d) $\lambda_T = 1{,}0.10^{-5}$ a too large value

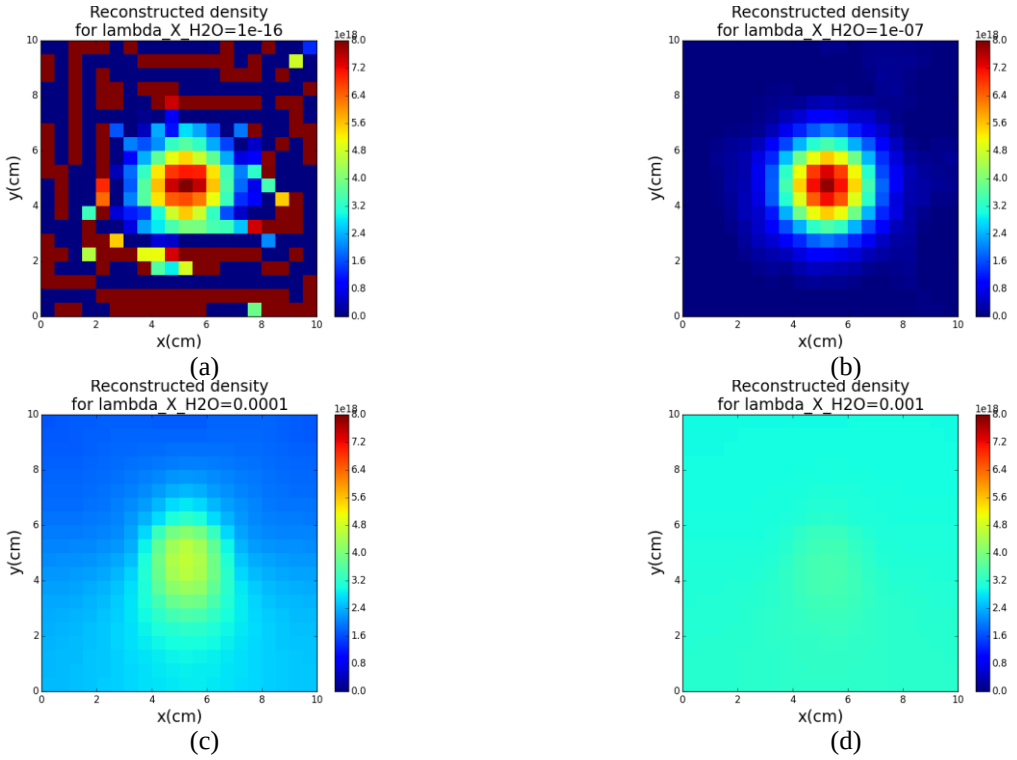

(a) (b) (c) (d)

Figure 12: Different results of tomographic reconstruction of the concentration of H_2O f the temperature with temperature fixed to the true value for different values of regularisation coefficient: (a) with $\lambda_{X_{H_2O}} = 1{,}0.10^{-16}$ a too low values, (b) $\lambda_{X_{H_2O}} = 1{,}0.10^{-7}$ the optimal value, (c) $\lambda_{X_{H_2O}} = 1{,}0.10^{-4}$ and (d) $\lambda_{X_{H_2O}} = 1{,}0.10^{-3}$ too large value

DOI: 10.13009/EUCASS2019-482

These results show that it is possible to reconstruct temperature or density profiles separately if the other is known and fixed by choosing the optimal regularisation coefficient. However, in a real case, the two profiles need to be rebuilt simultaneously. But in this case we have found that the couple $\left(\lambda_{X_{H_2O}}, \lambda_T\right)$ that have been found by the two separate errors curves are not the optimal ones. Indeed, the resolution of the inverse problem by equation (8) gives the results of the Figure 13 which are not as good as the ones obtained separately.

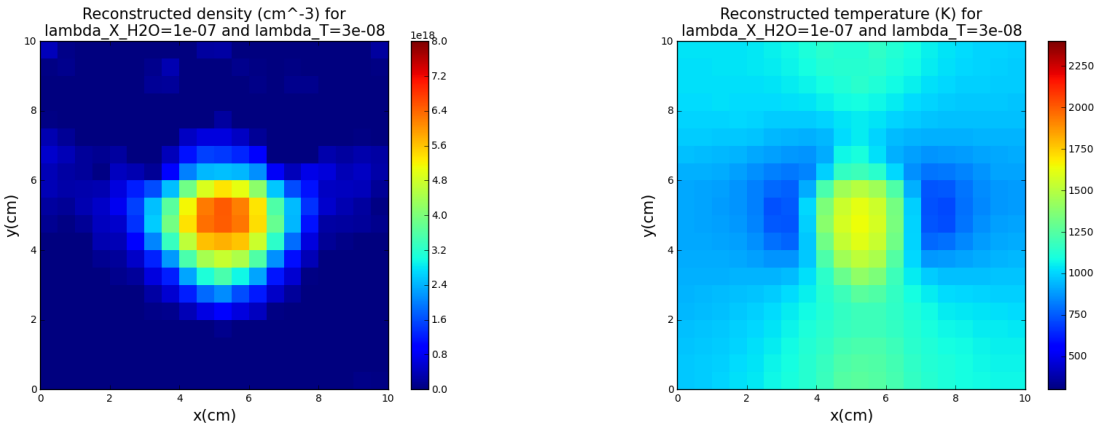

(a) (b)

Figure 13: Results of tomographic rebuilt of (a) H_2O density and (b) temperature by using the two optimal regularisation coefficients $\left(\lambda_{X_{H_2O}}, \lambda_T\right)$ found by the L-curve method

As a results, we conclude that the separate optimisation is not accurate enough to choose an optimal couple $\left(\lambda_{X_{H_2O}}, \lambda_T\right)$ for the complete calculation. So, it is necessary to find a way to optimise the couple $\left(\lambda_{X_{H_2O}}, \lambda_T\right)$ simultaneously in order to take into account the mutual influence on the spectra of temperature and H_2O density. As a result, we decide to optimize it by a parametric approach. The idea is to use the results of the reconstruction error curves from Figure 10 to do a first approximation of each optimal regularisation coefficient. After that, we choose for the couple $\left(\lambda_{X_{H_2O}}, \lambda_T\right)$ two ranges around the first approximation of regularisation coefficients . The optimisation consists to do tomographic reconstruction of H_2O density and temperature simultaneously for several couple $\left(\lambda_{X_{H_2O}}, \lambda_T\right)$ in the specified range, and to calculate for each of them a sum of relative difference with the two ground truth profiles:

$$D_{gt} = \frac{\left\| X_{H_2O_{gt}} - T_{rec} \right\|^2}{\left\| X_{H_2O_{gt}} \right\|^2} + \frac{\left\| T_{gt} - T_{rec} \right\|^2}{\left\| T_{gt} \right\|^2} \tag{12}$$

As a result, it is possible to draw a map of relative difference D_{gt} as a function of $\lambda_{X_{H_2O}}$ and λ_T like represented on the Figure 14. The couple that gives the weakest value of D_{gt} is the optimal couple to choose.

DOI: 10.13009/EUCASS2019-482

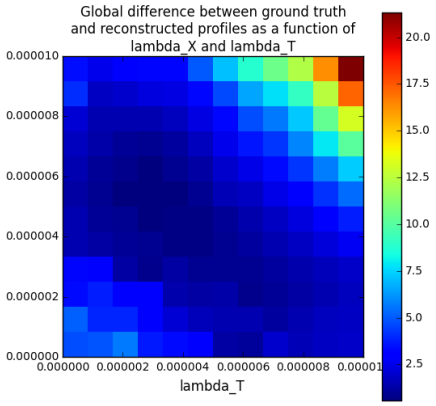

Figure 14: Representation of the difference D_{gt} as a function of $\lambda_{X_{H_2O}}$ and λ_T

According to the Figure 14, the best couple of regularisation coefficients is $\lambda_{X_{H_2O}} = 3{,}0.10^{-9}$ and $\lambda_T = 1{,}0.10^{-9}$. They are not the same than the ones calculated with independent error minimisation. If we draw the results for tomographic reconstruction with these coefficients, the results are the ones shown on the Figure 15.

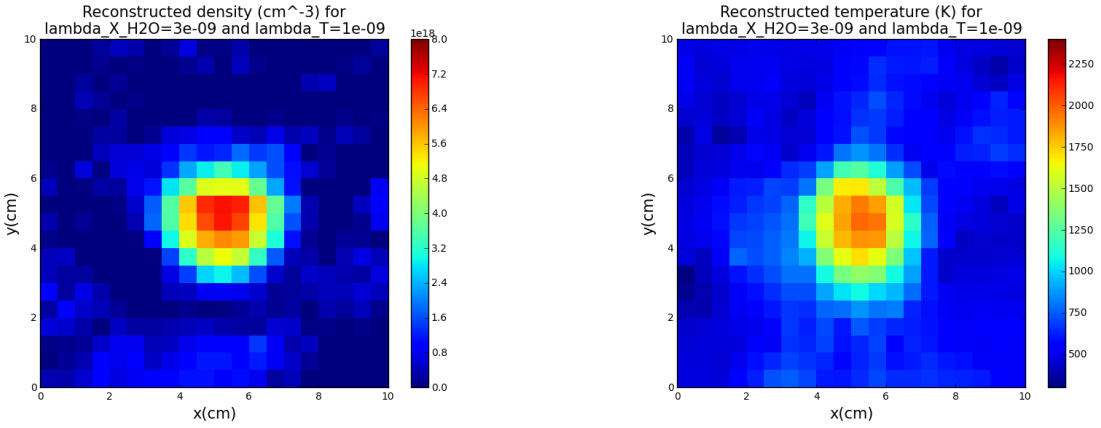

(a) (b)

Figure 15: Tomographic reconstruction of (a) H_2O density and (b) temperature profiles with the optimal couple$\left(\lambda_{X_{H_2O}}, \lambda_T\right)$

So, this numerical study has shown that it is necessary to optimize the two regularisation parameters in the same time to obtain a good couple of $\left(\lambda_{X_{H_2O}}, \lambda_T\right)$. However, these operations are not possible on experimental spectra because the ground truth profiles are not known. As a result, the future work is to find a way to optimize the two regularisations parameters only with experimental data.

6. Tomographic reconstruction on experimental spectra

In this part we will present an application of the tomographic algorithm on experimental spectra acquired on a MacKenna burner. The beam arrangement is that of Figure 8 (b). The hypotheses of constant atmospheric pressure and with no CO_2 visible in the flame are kept on this case of reconstruction. The tomographic reconstruction involves H_2O density and temperature. A lot of experimental problems have been met during this experiment and the spectral calibration processing. Indeed, the first problem is the large noise amount on the spectra. The second is the envelop suppression that deforms the line shape on some spectra (Figure 16 (a)). The shape of these lines can induce error on sought parameters and in particular on the temperature which is very dependent on the line shape. Moreover, due to suppression of the atmospheric contributions the spectra acquired outside the flame like Figure 16 (a) should appear

DOI: 10.13009/EUCASS2019-482

flat. The fluctuations visible on Figure 16 could be interpreted by the algorithm like some kind of absorption and bias the estimation. So, it has been necessary to perform pre-processing before the tomographic reconstruction.

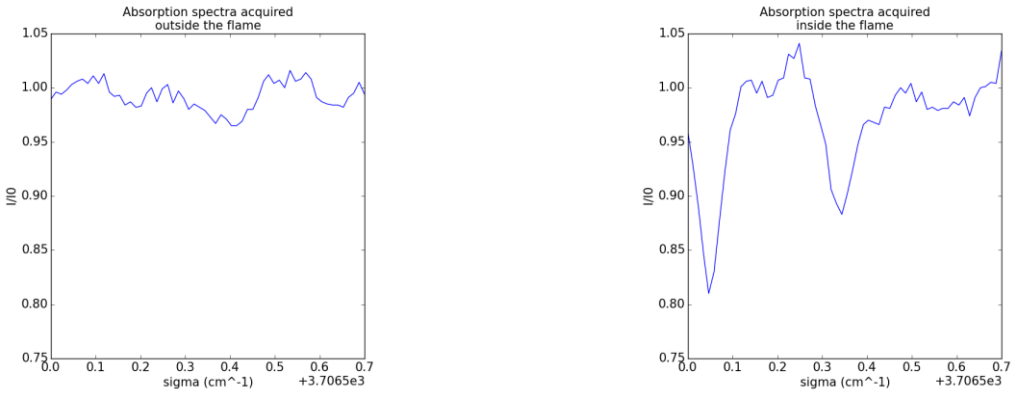

(a) (b)

Figure 16: Example of two spectra acquired in the region of interest with (a) a spectra outside the flame and (b) inside the flame

The first operation is to fit a rough template of the flame to the spectra. The template consists of top hat profiles of temperature or concentration. The diameter of the top-hat is fixed to 6cm, i.e. the diameter of the MacKenna burner. Location of top-hat centre, temperature and concentration inside top hat are free parameters that are fitted in the least squared sense to the measured spectra by minimization of score $M(10)$. The intensities and positions of the two disks that give the best data fit are represented on Figure 17.

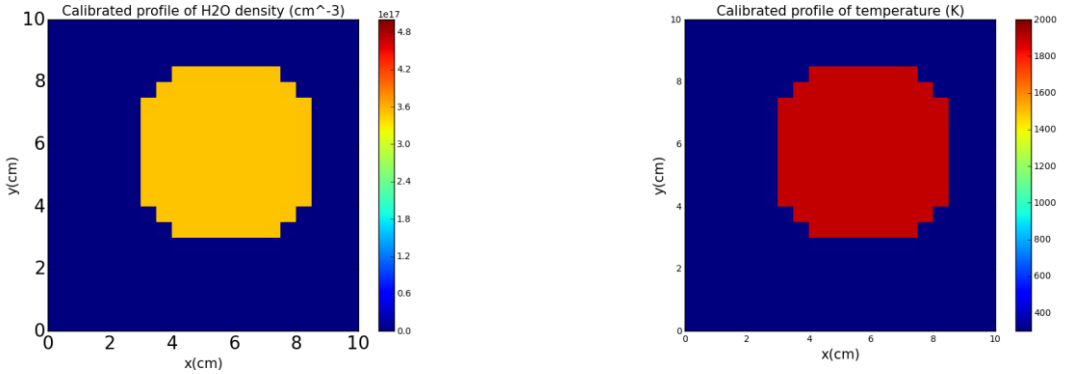

(a) (b)

Figure 17: Calibrated profiles of (a) H_2O density and (b) temperature that gives the best data fitting

These figures show that the flame is not positioned at image centre as it was expected. This shift is a consequence of inaccurate positioning of the metallic crown around the flame. The temperature inside this disk is 1900 K which corresponding of the expected value in this kind of burner. This data fitting is illustrated on Figure 18 that represents the two acquired spectra of Figure 16 in superposition to the same that are simulated through the template profiles. We can see on these two examples that these profiles give a good first approximation of a flame shape according to measured data.

DOI: 10.13009/EUCASS2019-482

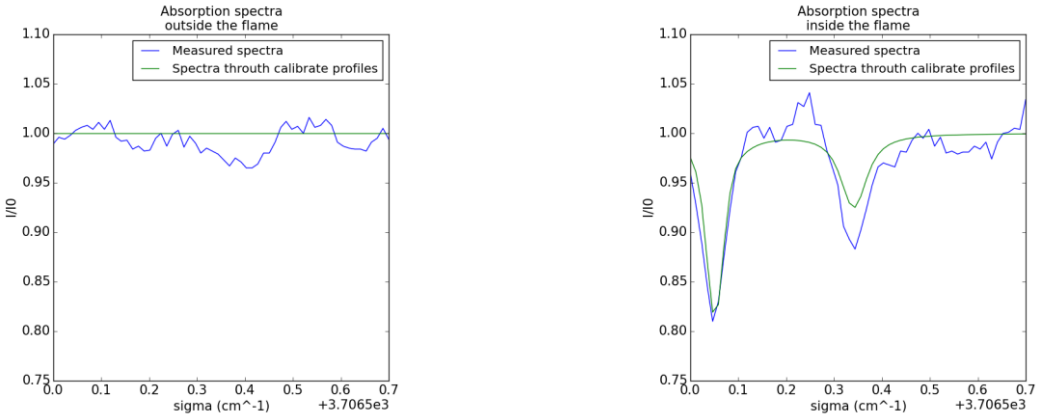

(a) (b)

Figure 18: Spectra acquired and given through the calibrated profiles in the region of interest with (a) a spectra outside the flame and (b) inside the flame

The tomographic algorithm on the experimental data is then initialized with the profiles of Figure 17 with a correct pair of $\left(\lambda_{X_{H_2O}}, \lambda_T\right)$. This pair of regularisation parameters has been obtained by manual tuning around values of $\left(\lambda_{X_{H_2O}}, \lambda_T\right)$ found by simulations (Figure 15). We observed the reconstructed results and compared it with the expected shape of the density and temperature profiles to choose the best regularisation parameters pair. The best pair gives the results represented on Figure 19. As a result, the tomographic algorithm modifies the two template profiles in order to provide a best fitting of the data.

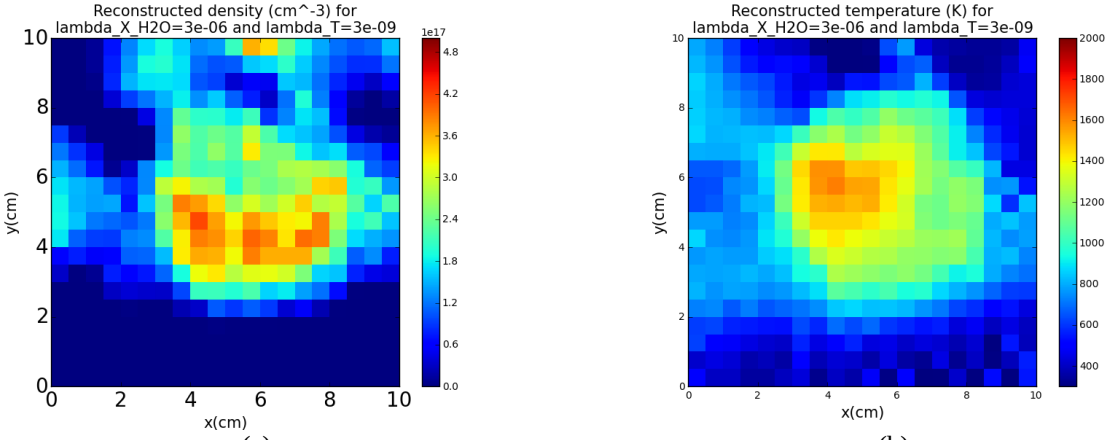

(a) (b)

Figure 19: Tomographic reconstruction *with* $\lambda_{X_{H_2O}} = 3{,}0.10^{-6}$ and $\lambda_T = 3{,}0.10^{-9}$ of (a) H_2O density and (b) temperature on experimental spectra

The fitted spectra obtained with these profiles are represented on Figure 20. It is show that the spectra after tomographic optimisation have been changed and at the same time they have decrease the criterion of equation (6) and the residual of equation (10). The data fit is better than the one done only with the two H_2O density and temperature top-hat profiles.

DOI: 10.13009/EUCASS2019-482

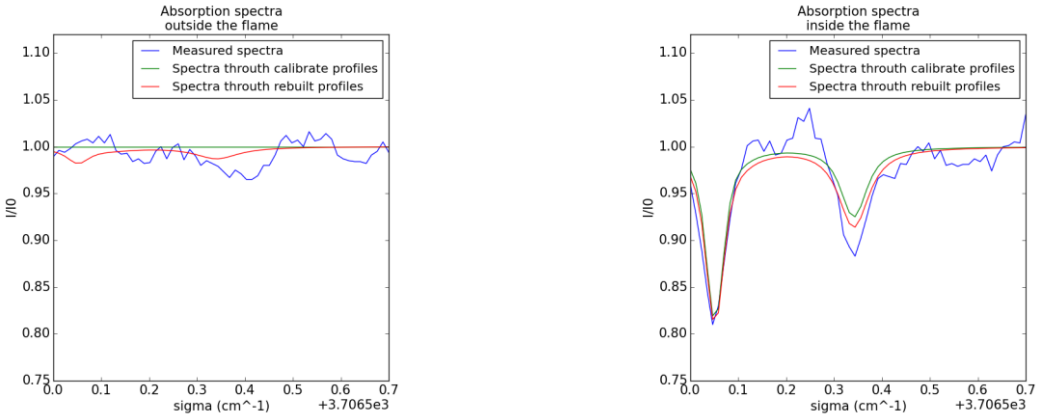

(a) (b)

Figure 20: Measured spectra , given through the calibrated and the rebuilt profile in the region of interest with (a) a spectra outside the flame and (b) inside the flame

By observation of the results of the Figure 19, the global shape of the MacKenna burner is respected. On the contrary of the template profiles, this reconstruction makes adjustment of this shape and shows some fluctuations inside the flame. On the other hand, some obvious errors are visible with the presence of H_2O at the boundary of the domain, and large temperature at some points outside the flame. It is probably come from some kind of over-smoothing of the solution by the regularisation. So, in this case where the data are deteriorated by noise and residuals of the spectral envelop suppression, the data are not as reliable as it is needed. So the regularisation effect must be increase to process correctly the data but it has an effect to over-smooth the result.

As a result, in case of large measurements error, the tomographic reconstruction should be tuned not to fit too closely to the data. In this case, it is important to optimise correctly the regularisation parameters to compensate these errors. Conversely, the regularisation must not be too important in order to avoid over-smoothing of the solution. As a conclusion, a compromise must be found to between the data fit and the regularisation and so it is necessary to study in depth a protocol to optimize the regularisation parameters with experimental data.

Conclusion

We have proposed a TDLAT method based on an iterative least-squares optimization of a regularized criterion. This method has been studied both numerically and experimentally on a test case involving a McKenna burner and a scanning multi-line spectrometer.

On the experimental aspect, we have observed that the calibration process is an important source of systematic errors. This step needs to be improved in order to have better projected spectra required for a detailed reconstruction. In this line, it could be important to derive a precise model of the envelop suppression operation on the measured signal and to characterize more precisely the effect of noise on absorption lines.

On the algorithmic aspect, our method gives satisfactory results when knowing the regularization parameters and an initial guess. Improvements may concern the search for the regularisation parameters in a multi-dimensional problem, ie. involving density, pressure and temperature reconstruction simultaneously, which is, besides, nonlinear. On the simulation study, we have tried to implement a parametric method to improve the parameters using the norm of the difference of the reconstructed profiles with respect to ground truth profiles. Still, simulation is not able to reproduce the degradations of the signal that occur in a real experiment; hence the estimated parameters are not directly usable in experiments. Classical method for choosing the parameter such as the L-curve seem not well adapted to the problem. Hence the automatic tuning of the regularization parameters in real data processing is, in our opinion, still an open issue.

The perspectives of this work are an improvement of the tomographic algorithm and of the acquisitions techniques. In a more long term, the objective is to implement the experimental device and the algorithm on turbulent flames and to add the reconstruction of the pressure in the algorithm and the way to be able to study several chemical species in the flames.

DOI: 10.13009/EUCASS2019-482

References

[1] M. P. Arroyo et R. K. Hanson, « Absorption measurements of water-vapor concentration, temperature, and line-shape parameters using a tunable InGaAsP diode laser », *Appl. Opt.*, vol. 32, n° 30, p. 6104–6116, 1993.
[2] L. S. Rothman *et al.*, « THE HITRAN MOLECULAR SPECTROSCOPIC DATABASE AND HAWKS (HITRAN ATMOSPHERIC WORKSTATION): 1996 EDITION », *J. Quant. Spectrosc. Radiat. Transf.*, vol. 60, n° 5, p. 665‑710, nov. 1998.
[3] A. K. Hui, B. H. Armstrong, et A. A. Wray, « Rapid computation of the Voigt and complex error functions », *J. Quant. Spectrosc. Radiat. Transf.*, vol. 19, n° 5, p. 509–516, 1978.
[4] K. T. Ladas et A. J. Devaney, « Generalized ART algorithm for diffraction tomography », *Inverse Probl.*, vol. 7, n° 1, p. 109, 1991.
[5] W. Cai et C. F. Kaminski, « Tomographic absorption spectroscopy for the study of gas dynamics and reactive flows », *Prog. Energy Combust. Sci.*, vol. 59, p. 1‑31, mars 2017.
[6] A. Guha et I. Schoegl, « Tomographic laser absorption spectroscopy using Tikhonov regularization », *Appl. Opt.*, vol. 53, n° 34, p. 8095, déc. 2014.
[7] P. C. Hansen, « Analysis of Discrete Ill-Posed Problems by Means of the L-Curve », *SIAM Rev.*, vol. 34, n° 4, p. 561‑580, déc. 1992.